International Journal of Materials Science and Applications
2013; 2(1) : 30-36
Published online January 10, 2013 (http://www.sciencepublishinggroup.com/j/ijmsa)
doi: 10.11648/j.ijmsa.20130101.14

Synthesis and Thermoelectric Study of Sb (III) Doped $Bi_2(Te_{1-x}Se_x)_3$ Thin Films by APT

S. M. Patil*, M. M. Salunkhe, N. B. Pawar, P. N. Bhosale

Materials Research Laboratory, Department of Chemistry, Shivaji University, Kolhapur-416 004

Email address:
sanjeevanipatil01@gmail.com (S. M. Patil)

To cite this article:
S. M. Patil, M. M. Salunkhe, N. B. Pawar, P. N. Bhosale. Synthesis and Thermoelectric Study of Sb (III) Doped $Bi_2(Te_{1-X}se_x)_3$ Thin Films by Apt, *International Journal of Materials Science and Applications.* Vol. 2, No. 1, 2013, pp. 30-36. doi: 10.11648/j.ijmsa.20130201.14

Abstract: Thermoelectric study of Sb (III) doped bismuth tellurium selenide ,Bi_{2-x} $Sb_x(Te_{1-x}Se_x)_3$ thin films were done.They are deposited by Arrested Precipitation Technique (APT). These thin films were prepared using a complexing agent triethanolamine (TEA) and a reducing agent sodium sulphite to avoid hydroxide formation of bismuth precursor Bi $(NO_3)_3$ and antimony precursor ($SbCl_3$) in aqueous medium to favor the reaction with Te^{2-} and Se^{2-}chalcogen ions. The preparative conditions such as pH, concentration of precursors, temperature, rate of agitation and time were finalized at initial stages of deposition. As deposited films were annealed at constant temperature (373K) in muffle furnace and then characterized for optostructural, morphological, thermoelectric and figure of merit (ZT). The results demonstrate that the Bi_{2-x} $Sb_x(Te_{1-x}Se_x)_3$ thin films prepared by APT shows band gap in the range 1.46eV to 1.89eV. X-Ray Diffraction (XRD) pattern, Scanning Electron Microscopy (SEM) images reveals that Bi_{2-x} $Sb_x(Te_{1-x}Se_x)_3$ mixed metal chalcogenide films are of nanocrystalline nature and have rhombohedral structure and better morphology. EDAX study shows good stoichiometry. Electrical and TEP study shows Sb(III) doping in $Bi_2(_{Te1}$-$xSe_x)_3$ mixed metal chalcogenide thin films are semiconducting having p-type conduction mechanism. The highest figure of merit obtained was 0.312 and 0.569 for D1 to D5 samples.

Keywords: APT, Metal chalcogenides, X-ray diffraction, XPS

1. Introduction

Thermoelectric material has attracted a great deal of interest in the past decade for its potential application in energy conversion, solid-state refrigerating and cooling [1-2] based on the Seebeck effect, such as thermal sensors, hyper frequency power sensors, thermopiles, and wide-band radiation detectors. To improve the efficiency of thermoelectric devices, the appropriate thermoelectric materials having the best performance at a specific operating temperature must be selected. The thermoelectric figure of merit, ZT, can be expressed as S2 T /ρ.κ, where S is the Seebeck coefficient, ρ the electrical registivity, T the temperature, and κ the thermal conductivity. Present state-of-the-art thermoelectric materials show a figure-of-merit (ZT) around unity. Sb (III) doped bismuth tellurium selenide with a rhombohedral crystal structure has been discovered to study its power generation applications.

Various methods of preparations of mixed Sb_2Te_3, Bi_2Te_3, Bi_2Se_3, Sb_2Se_3 thin films have been reported such as solvothermal [3], Electrodeposition [4], The pulsed magnetron sputtering [5], and also alloys of V-VI group reported by Lukyanova and Kutasov [6-8] etc reported hot extruded $(Bi,Sb)_2(Te,Se)_3$ alloys for advanced thermoelectric modules. Further these are prepared by ion beam sputtering [9], Sceen printing [10] and Thermal vacuum evaporation [11]. Many researchers working on binary, ternary and quaternary semiconducting compounds of V and VI group elements, particularly chalcogenides of bismuth, antimony and arsenic. Hence in the present investigation Sb is doped in the ternary $Bi_2(Te_{1-x}$ $Se_x)_3$ thin films by arrested precipitation technique (APT) and effects are studied [12,13].

2. Experimental

2.1. Preparation of Sb (III) Doped Bi2 (Te1-Xsex)3 Thin Films

Sb (III) doped $Bi_2(Te_{1-x}$ $Se_x)_3$ mixed metal chalcogenide thin films were prepared by keeping constant amount of the 15 ml sodium tellurium sulphite, 15 ml sodium seleno sulphite (Na_2SeSO_3) for the sources of Te^{2-}, Se^{2-} respectively. Concentrations of Bi-TEA complex and Sb-TEA complex were varied in a volume stoichiometric ratio so as to obtain various compositions of Sb (III) doped $Bi_2(Te_{1-x}$ $Se_x)_3$thin

films. Deposition of mixed Sb (III) doped $Bi_2(Te_{1-x}Se_x)_3$mixed metal chalcogenide thin films was carried out by keeping all the parameters similar to those finalized for the $Bi_2(Te_{1-x}Se_x)_3$thin films. Table 1. shows film composition, the variations of Bi^{3+},Sb^{3+} ,Te^{2-} and Se^{2-} in Sb (III) doped $Bi_2(Te_{1-x}Se_x)_3$, their nomenclature, bath composition. Preparative conditions for the Sb (III) doped $Bi_2(Te_{1-x}Se_x)_3$thin films are pH= 10.5 ± 0.3,Temperature= 55 ± 0.5 0C, Deposition time = 2 hrs, Substrate rotation = 45 ± 5 rpm. Thickness of the film is in between 0.19 μm to 0.80 μm.

***Table 1**. Composition of the sample for deposition of Sb (III) doped $Bi_2(Te_{1-x}Se_x)_3$ thin films.*

Sample No.	Composition	Bath composition
D_1	$Bi_{1.98}Sb_{0.02}(Te_{0.5}Se_{0.5})_3$	(20 –x) ml 0.05 M Bi-TEA + x ml 0.05 M Sb-TEA + 15 ml 0.05 M Na_2TeSO_3 +15ml 0.05M Na_2SeSO_3 and rest is water to make 100 ml total volume. x is varied from 0.0 to 0.1 ml
D_2	$Bi_{1.96}Sb_{0.04}(Te_{0.5}Se_{0.5})_3$	
D_3	$Bi_{1.94}Sb_{0.06}(Te_{0.5}Se_{0.5})_3$	
D_4	$Bi_{1.92}Sb_{0.08}(Te_{0.5}Se_{0.5})_3$	
D_5	$Bi_{1.90}Sb_{0.1}(Te_{0.5}Se_{0.5})_3$	

2.2. Growth Mechanism of $Bi_2(Te_{1-x}Se_x)_3$Thin Film Formation

Arrested precipitation technique is suitable for the deposition of Sb (III) doped $Bi_2(Te_{1-x}Se_x)_3$ mixed type thin films. In the present investigation, we have slightly modified the chemical deposition method using polydentate chelating agent such as triethanolamine [N $(CH_2\text{-}CH_2\text{-}OH)_3$] as a complexing agent to arrest Bi^{3+} and Sb^{3+} ions. Organic complexing agent TEA have strong affinity towards the Bi^{3+} and Sb^{3+} ions and it's tendency to keep the Bi^{3+} and Sb^{3+} ion arrested in a solution even in alkaline pH range where the metal hydroxide formation is possible. Here ionic species of Bi^{3+}, Sb^{3+}, $Te^{2-}$and Se^{2-} are produced as per the following reaction equilibria.

Bi^{3+}, Sb^{3+}, Te^{2-} and Se^{2-} ions are slowly releases in the solution in an aqueous alkaline medium deposition of Sb(III) doped $Bi_2(Te_{1-x}Se_x)_3$ is takes place. The formation of Sb (III) doped $Bi_2(Te_{1-x}Se_x)_3$ thin films occurs when ionic product of Bi^{3+}, Sb^{3+}, Te^{2-} and Se^{2-} exceeds the solubility product of Sb (III) doped $Bi_2(Te_{1-x}Se_x)_3$. Overall growth mechanism of the mixed composites of bismuth antimony tellurium selenide is summarized as follows.

$$(NH_4)_3[Bi_2N(CH_2\text{-}CH_2\text{-}O)_3] + 6H_2O \rightarrow Bi^{3+} + 3NH_4OH + 3OH^- + 2[N(CH_2\text{-}CH_2\text{-}OH)_3] \quad (1)$$

$$(NH_4)_3[Sb_2N(CH_2\text{-}CH_2\text{-}O)_3] + 6H_2O \rightarrow Sb^{3+} + 3NH_4OH + 3OH^- + 2[N(CH_2\text{-}CH_2\text{-}OH)_3] \quad (2)$$

$$Na_2TeSO_3 + OH^- \rightarrow Na_2SO_4 + HTe^- \quad (3)$$

$$HTe^- + OH^- \rightarrow H_2O + Te^{2-} \quad (4)$$

$$Na_2SeSO_3 + OH^- \rightarrow Na_2SO_4 + HSe^- \quad (5)$$

$$HSe^- + OH^- \rightarrow H_2O + Se^{2-} \quad (6)$$

The reactions given in equation (1) to (6) shows that the Bi^{3+}, Sb^{3+}, Te^{2-} and Se^{2-} are condenses ion by ion basis on the glass substrate at pH 10.5 and 55°C temperature as follows:

$$Bi^{3+} + Sb^{3+} + nNa_2TeSO_3 + nNa_2SeSO_3 \rightarrow Bi_{2-x}Sb_x(Te_{1-x}Se_x)_3 + nNa_2SO_4 + n(TEA) \quad (7)$$

Finally, the deposited Sb (III) doped $Bi_2(Te_{1-x}Se_x)_3$ films prepared by arrested precipitation technique are found to be uniform and well adherent to the substrate.

3. Result and Discussion

3.1. UV-Visible Spectroscopic Study

The optical absorption coefficient (α) of Sb (III) doped $Bi_2(Te_{1-x}Se_x)_3$ is found to be in the order of 10^5 cm^{-1}. The dependence of the optical absorption on the photon energy is described by the relation,

$$\alpha = \frac{A}{h\nu}(h\nu - Eg)^n \quad (8)$$

$(\alpha h\nu)^2$ vs hν for Sb (III) doped $Bi_2(Te_{1-x}Se_x)$ having different composition was plotted and the values of the optical band gap E_g were taken as the intercept of $(\alpha h\nu)^2$ vs hν on energy axis at α=0 as shown in Figure 1. The estimated values of E_g of different composition of Sb (III) doped $Bi_2(Te_{1-x}Se_x)_3$ films are listed in Table 3 The substitution of 'Sb' atoms by 'Bi' atoms in $Bi_2(Te_{1-x}Se_x)_3$ thin films results in increasing the optical band gap of the system. The increasing in band gap is caused by alloying effect. This effect causes changes in bond angles and/or bond lengths. The same observation was found by M. M. El-Samanoudy for replacement of Sb atoms by Bi atoms in case of $Ge_{25}Sb_{15-x}Bi_xS_{60}$ thin films [14]. From Figure 2 the type of transition is direct and allowed. It was found that the optical energy gap E_g increases gradually from 1.46 eV to 1.89 eV with increasing Sb in 0.02 % to 0.1 %. SEM micrograph shows decrease in grain size which is evidence for the increase of band gap with Sb doping concentration. Another reason is antimony atoms (1.33 A^0) are smaller than bismuth atoms (1.43 A^0) and possess lower-energy atomic orbital, which can lead to wider energy gap by lowering top of the valence band and more importantly raising the bottom of the conduction band. Also vary small grain size (nanometer size) could shift the band gap to higher values compared with the bulk crystalline value [15].

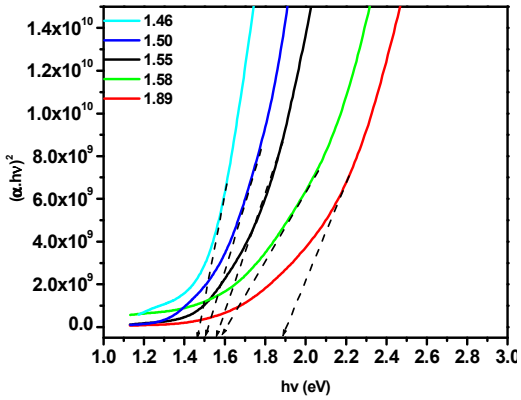

Figure 1. *Plot of $(\alpha h\nu)^2$ vs $h\nu$ for Sb (III) doped $Bi_2(Te_{1-x}Se_x)_3$ thin films.*

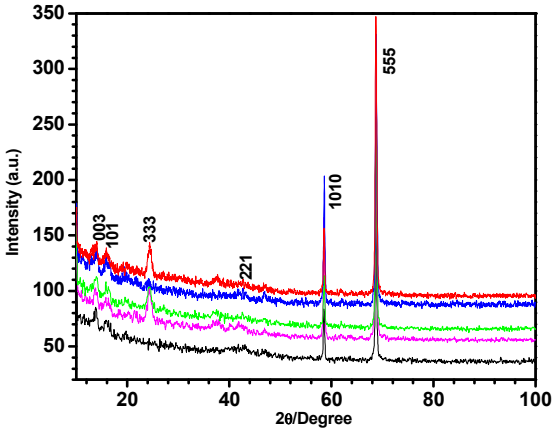

Figure 2. *XRD pattern of Sb (III) doped $Bi_2(Te_{1-x}Se_x)_3$thin.*

Table 3. *Variation of band gap for Sb (III) doped $Bi_2(Te_{1-x}Se_x)_3$ thin films.*

Film composition	Band Gap (Eg) eV
$D_1 = Bi_{1.98}Sb_{0.02}(Te_{0.5}Se_{0.5})_3$	1.46
$D_2 = Bi_{1.96}Sb_{0.04}(Te_{0.5}Se_{0.5})_3$	1.50
$D_3 = Bi_{1.94}Sb_{0.06}(Te_{0.5}Se_{0.5})_3$	1.55
$D_4 = Bi_{1.92}Sb_{0.08}(Te_{0.5}Se_{0.5})_3$	1.58
$D_5 = Bi_{1.90}Sb_{0.1}(Te_{0.5}Se_{0.5})_3$	1.89

3.2. X-ray Diffraction (XRD) Study

X- ray diffraction (XRD) analysis was carried out for all samples using a Philips PW-1710 X-ray diffractometer for the 2θ ranging from 10^0 to 100^0 with Cr K_α line used as a beam (λ=2.25 A^0). XRD pattern of the doped thin films are shown in Figure 2 From the XRD pattern it is seen that thin film shows nanocrystalline nature. All Sb (III) doped $Bi_2(Te_{1-x}Se_x)_3$ shows a rhombohedral structure. The comparison of the observed 'd' values and the crystallite size of the film calculated using Debye Scherrer formula of the deposited samples are given in Table 2.

Doped thin films having different composition (x =0.2 to 0.1 ml) deposited at 55 ^oC. The presence of most intense diffraction peaks at (555), (1010), (003), (101), (333) and (221) were found. The plane indices are obtained by comparing the intensities and positions of the peaks with those of Bi_2Se_3, Bi_2Te_3, Sb_2Se_3 and Sb_2Te_3, which are given by JCPDS file no.85-0519, 85-0439, 75-1462, 72-1990, etc. films.

The strongest peak for all films occurred at 2θ = 68.78^o with d = 2.02A^o. From the crystalline size (D) of the deposited thin films it reveals that intensity of the peak decreases with doping of Sb (III) and broadening of small peaks. This attributed to the fact that there might be decrease in crystallite size on Sb (III doping in $Bi_2(Te_{1-x}\ Se_x)_3$ thin films; also small degree of broadening occurs as a result of increase in strain in the film due to Sb incorporation in the Bi lattice site. Careful observation of the XRD pattern of the films shows that some peaks are remained unchanged and some new lines appeared in the pattern. The increase in the number of new peaks are due to introduction of new planes because of Sb(III), caused by non uniform distortion as a result of doping [10].

Table 2. *XRD results of the Sb (III) doped $Bi_2(Te_{1-x}Se_x)_3$ thin films for various compositions.*

Film Composition	Observed 'd' value (A^o)	JCPDS 'd' values A^o		Crystallite size 'D' (nm)
		'd'(A)	(hkl)	
	9.44	9.43	003	
	5.40	8.02	333	
$D_1=Bi_{1.98}Sb_{.02}(Te_{0.5}\ Se_{0.5})$	2.34	2.34	343	42.13
	2.02	2.02	413	
	1.57	1.58	224	
	9.96	9.96	003	
	8.28	5.07	101	
$D_2=Bi_{1.96}Sb_{.04}(Te_{0.5}\ Se_{0.5})$	5.07	2.41	201	41.67
	2.34	2.34	101	
	2.02	2.02	503	
	9.50	9.96	003	
	5.45	5.07	335	
	2.87	2.87	221	
$D_3=Bi_{1.94}Sb_{.06}(Te_{0.5}\ Se_{0.5})$	2.34	2.34	403	39.89
	2.16	2.16	205	
	2.10	2.07	343	
	2.02	2.02	413	
	8.28	9.96	101	
$D_4=Bi_{1.92}Sb_{.08}(Te_{0.5}\ Se_{0.5})$	5.47	5.07	222	39.38
	3.52	3.58	012	

	3.14	3.13	015	
	2.88	2.89	221	
	2.33	2.33	304	
	2.21	2.23	443	
	2.02	2.02	413	
	1.80	1.80	131	
	9.40	8.28	003	
	5.43	5.07	222	
D_5=$Bi_{1.90}Sb_{.1}$ ($Te_{0.5}$ $Se_{0.5}$)	2.34	3.58	403	39.36
	2.02	3.13	555	
	1.57	2.89	0210	

3.3. Scanning Electron Microscopic (SEM) Study

Scanning electron micrograph of Sb (III) doped $Bi_2(Te_{1-x}Se_x)_3$ at 10000 X magnification is shown in Figure 3 The SEM micrographs shows well adherent, smooth and uniform film surface without cracks under low magnification which accounts high mechanical stability of the samples. We have observed significant variation in the morphological properties of the films for the variation of Sb doping.

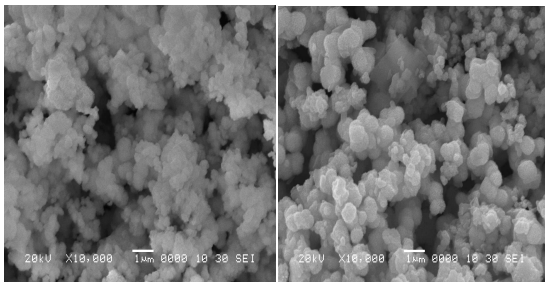

(a) D_1 **(b) D_2**

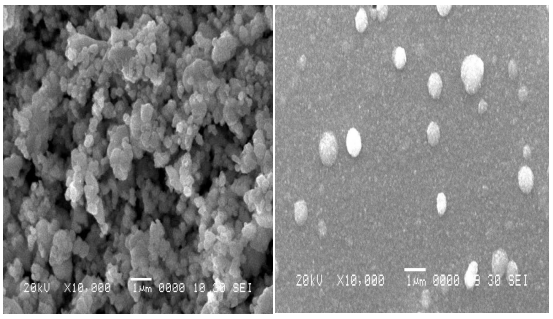

(c) D_3 **(d) D_4**

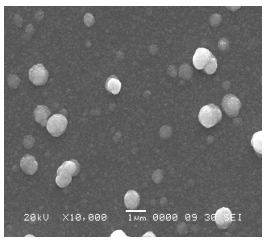

(e) D_5

Figure 3. *SEM micrographs for Sb (III) doped $Bi_2(Te_{1-x}Se_x)_3$ thin films.*

After doping Sb(III) slightly cross linked grains coalesce and aggregates of crystallites are formed .In some regions overgrowth were also observed. It shows the co-existence of small and relatively large grains on the film surface. Figure 3 $D_1$to D_5 shows that large crystallites are broken to well define nanocrystalline particles with fine background as a result of further antimony (III) doping. These micrographs reveal that the grain size decreases, as the concentration of doping of Sb (III) increases. The result of increase in Sb doping indicating that Sb is grain growth inhibitor in $Bi_2(Te_{1-x}Se_x)_3$ films. Grain size was determined using the linear intercept technique.

The grain size of the antimony (III) doped Bi_2 $(Te_{0.5}Se_{0.5})_3$ thin films with x= 0.02, 0.04, 0.06, 0.1 are 650 nm, 548nm, 398nm 267nm and 140 nm respectively. These results are consistent with the XRD results which also show broadening of peaks as a result of antimony (III) doping indicating decrease of crystalline size [16].

3.4. Energy Dispersive X-ray Analysis (EDAX)

Compositional analysis of Sb (III) doped $Bi_2(Te_{1-x}Se_x)_3$ thin films was carried out by EDAX analysis. EDAX Images of few samples are shown in Figure 4. The doping (Sb) concentration in the starting solution was varied from 0.02% to 0.1%. The atomic percentage ratio of Bi, Sb, Te and Se in deposited thin films is listed in Table 4, it shows that the samples are in good stoichiometric ratio. Deviation from the atomic percentage of Bi, Sb, Se, and Te in Sb (III) doped $Bi_2(Te_{1-x}Se_x)_3$ could be attributed due to the presence of oxygen. Oxygen may be incorporated into the film either from the atmosphere or from the alkaline medium of the bath solution. In our chemical bath deposition experiment, the pH is maintained in alkaline condition and hence there is significant influence of OH^- ions on the deposition process, which favors the inclusion of oxygen in the deposited films, resulting in oxygen contamina tion. The excess of Sb bounded to oxygen and hydrogen in the form of $Sb(OH)_3$ and Sb_2O_3. Same type of conclusion was observed in XPS analysis [10]

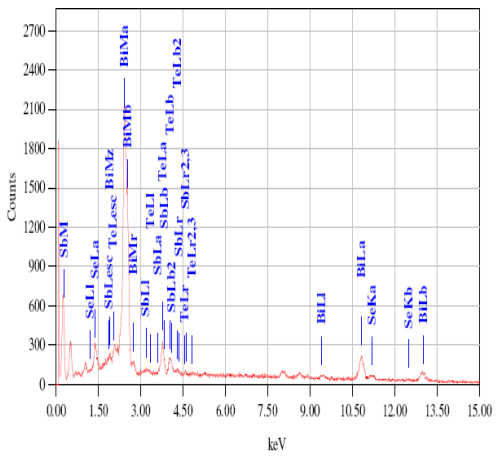

(a) D_1=$Bi_{1.98}Sb_{0.02}(Te_{0.5}Se_{0.5})_3$

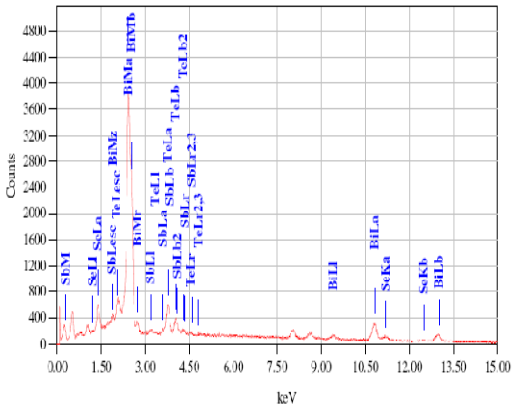

(b) $D_3=Bi_{1.94}Sb_{0.06}(Te_{0.5}Se_{0.5})_3$

Figure 4. *EDAX spectra of Sb (III) doped $Bi_2(Te_{1-x}Se_x)_3$ thin films.*

Table 4. *Quantitative analysis of Bi, Sb,Te and Se by using EDAX for Sb (III) doped $Bi_2(Te_{1-x}Se_x)_3$.*

Film composition	Elements	Atomic percentage	
		Observed	Expected
D_1 $Bi_{1.98}Sb_{0.02}(Te_{0.5}Se_{0.5})_3$	Bi	43.42	39.60
	Sb	0.45	0.40
	Te	26.85	30.00
	Se	29.28	30.00
D_2 $Bi_{1.96}$ $Sb_{0.04}(Te_{0.5}Se_{0.5})_3$	Bi	44.48	39.20
	Sb	0.89	0.80
	Te	26.70	30.00
	Se	27.93	30.00
D_3 $Bi_{1.94}$ $Sb_{0.06}(Te_{0.5}Se_{0.5})_3$	Bi	44.95	38.80
	Sb	1.28	1.20
	Te	27.00	30.00
	Se	26.77	30.00
D_4 $Bi_{1.92}$ $Sb_{0.08}(Te_{0.5}Se_{0.5})_3$	Bi	43.75	38.40
	Sb	1.66	1.60
	Te	27.50	30.00
	Se	27.09	30.00
D_5 $Bi_{1.90}$ $Sb_{0.10}(TSe_{0.5}Se_{0.5})_3$	Bi	42.98	38.20
	Sb	1.90	1.80
	Te	26.95	30.00
	Se	28.25	30.00

3.5. Thermoelectric Study of Sb (III) Doped Bi $_2(Te_{1-X}se_x)_3$ Thin Film

3.5.1. Electrical Conductivity

The electrical conductivity of the films was studied by using two point D. C. probe method. Electrical conductivity measurement was made in the temperature range 300 to 500 K at constant voltage (5 volt). The temperature dependence of electrical conductivity of the semiconducting thin films is given by equation

$$\sigma = \sigma_o \exp\left(\frac{-E_a}{kT}\right) \qquad (9)$$

The variation of $\ln\sigma$ with 1000 / T in the temperature range 300 to 500 K for as deposited and annealed samples were shown in Figure 5 From graph it reveals that electrical conductivity increases after Sb(III) doping in $Bi_2(Te_{1-x}$ $Se_x)_3$ thin films, indicating that all the films are semiconducting in nature. From the slope of linear plots, activation energies were calculated for two temperature region. The activation energies for low temperature region and in high temperature region were represented in Table 5. Sb doping produces resonance levels in the valence band of $Bi_{2-x}Sb_x(Te_{1-x}Sex)_3$ solid solutions, which results in fermi level pinning, thereby improving the electrical homogeneity of the crystals.

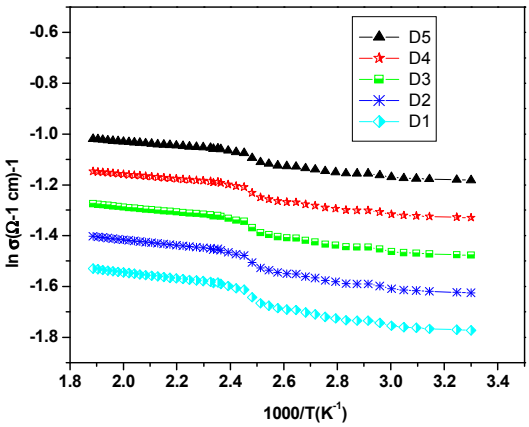

Figure 5. *The variation of $\ln\sigma$ with 1000/T for Sb (III) doped $Bi_2(Te_{1-x}Se_x)_3$ where x varied from 0.02 to 0.1%.*

Table 5*. Observed variation of activation energy (ΔE) for Sb (III) doped $Bi_2(Te_{1-x}Se_x)_3$ thin films.*

Composition of the films	High temperature region ΔE (eV)	Low temperature region ΔE (eV)
D_1:$Bi_{1.98}$ $Sb_{0.02}(Te_{0.5}Se_{0.5})_3$	0.02589	0.01667
D_2:$Bi_{1.96}$ $Sb_{0.04}(Te_{0.5}Se_{0.5})_3$	0.03145	0.01821
D_3:$Bi_{1.94}Sb_{0.06}$ $(Te_{0.5}Se_{0.5})_3$	0.03409	0.01958
D_4:$Bi_{1.92}Sb_{0.08}(Te_{0.5}Se_{0.5})_3$	0.03874	0.02048
D_5:$Bi_{1.90}Sb_{0.1}(Te_{0.5}Se_{0.5})_3$	0.04087	0.02250

Electrical conductivity in Sb-doped $Bi_2(Te_{1-x}Se_x)_3$ thin films as a function of Sb doping content. Undoped $Bi_2(Te_{1-x}Se_x)_3$ shows n-type property with quite a few of electrons and the number of electron decrease with increasing Sb doping content due to ionization of Sb dopants replaced at bismuth sites. Electron concentration decreases with Sb doping level from 0.02 to 0.1% Sb(III) doped $Bi_2(Te_{1-x}Se_x)$ thin film, the number of holes exceed that of

electrons and this film shows p-type conduction. Electrical resistivity increases with increasing Sb doping content because electron concentration decreases by compensation of excess electrons. Also the grain size becomes smaller and the developed surface of the grain boundaries increased. Consequently, carrier movement is disturbed by grain boundary scattering [17].

3.5.2. Thermal Electrical Power Measurement (TEP)

The Seebeck coefficient of the material was measured at 300 to 500K with digital Testronix-8 microvolt meter. Figure 6. shows Seebeck coefficients of annealed Sb (III) doped $Bi_2(Te_{1-x}Se_{0.5})_3$ D_1 to D_5 samples deposited by Arrested precipitation technique. From 0.02 to 0.1% Sb doping, the Seebeck coefficients indicate that all the films are p-type conduction. The simplest explanation for this behavior can be made by considering Sb atoms taking the place of Bi sites in the crystal lattice. They behave as acceptors and offset the donating effect of interstitial atoms. In this way, the electrical resistivity increases with increasing Sb doping concentration. The interstitial site occupations become higher and attain saturation at 0.1 % Sb doping. The measured curves of the Seebeck coefficient clearly show the inversion of electron-type conductivity to hole-type conductivity.

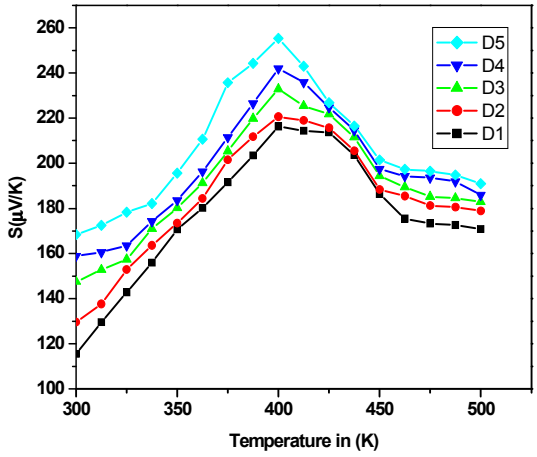

Figure 6. *Variation of thermo emf with temperature for Sb (III) doped $Bi_2(Te_{1-x}Se_x)_3$ where x varied from 0.02% to 0.1%.*

Seebeck coefficient increases more or less smoothly over the measured temperature region. The 'S' ranging from 115 to 168 μV/K at 300 K for Sb (III) doped $Bi_2(Te_{0.5}Se_{0.5})_3$ thin films for D_1 to D_5 samples. The Seebeck coefficient (S) increases in the series Bi_{2-x} $Sb_x(Te_{0.5}Se_{0.5})_3$ with increasing Sb content, until the maximum is reached at x=0.10 at 300 K. As Sb^{3+} have less electrons than Bi^{3+}, increase in Sb content in Bi_{2-x} $Sb_x(Te_{0.5}Se_{0.5})_3$ material increases hole concentration which results in increase in Seebeck coefficient [18]. The power factor is one of the important thermoelectric parameter, which determines the performance of the thermoelectric energy converters. The power factor is characterized by the formula $PF=(S^2/\rho)$, where S stand for Seebeck coefficient and ρ is the electrical resistivity. Table 6 shows the power factors of Sb(III) doped $Bi_2(Te_{0.5}Se_{0.5})_3$ thin films at room temperature. The power factor increases with increasing Sb doping concentration from 32.5 to 58.31$Wcm^{-1}K^{-2}$.

3.5.3. Thermal Conductivity

The thermal conductivity measurement with the help of CT–Meter [C-T meter (Teleph, France)] as discussed in chapter V at room temperature. It shows decrease in thermal conductivities from 0.391 to 0.255 W/mK for Sb (III) doped $Bi_2(Te_{1-x}Se_x)_3$. Figure 7 shows thermal conductivity % of Sb(III) doped in $Bi_2(Te_{1-x}Se_x)_3$.

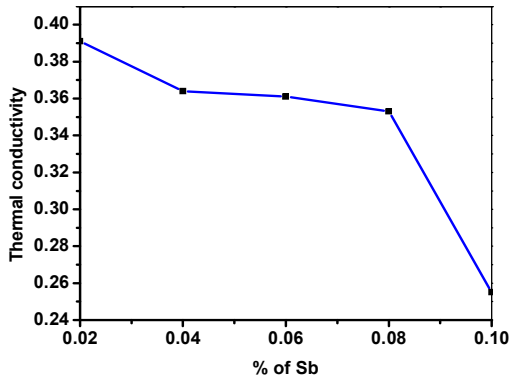

Figure 7. *Thermal conductivity with % Sb (III) doping in $Bi_2(Te_{1-x}Se_x)_3$.*

Thermoelectric performance (ZT)

Dimensionless figure of merit can be calculated by

$$Z\,T = \frac{S^2}{\rho\,.k} \times T \qquad (10)$$

The quality of thermoelectric materials is described by dimensionless figure of merit, ZT. Thermal conductivity was measured by different types of probes, namely cylindrical probe, two wire probe, iron probe and ring probe. Here we use ring probe CT meter. The ZT of the Sb (III) doped material was found to be about 0.312 to 0.569 at room temperature. The room temperature ZT values are shown in Table 6. Due to continued increase of the Seebeck coefficient in all samples, the power factor (S^2/ρ) and thermoelectric performance (ZT) increase substantially at higher temperatures [19]. Figure 8 shows the ZT value changes with percentage of Sb (III) dopent.

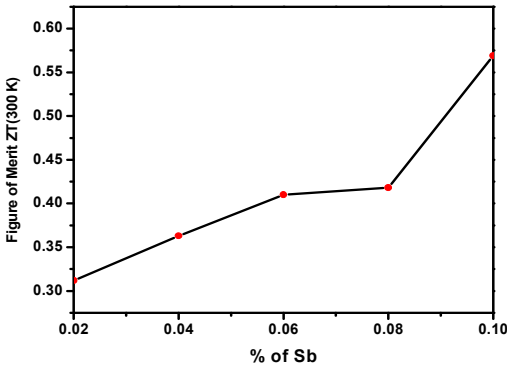

Figure 8. *Figure of Merit with % of Sb (III) doping in $Bi_2(Te_{1-x}Se_x)_3$.*

***Table 6**. Thermoelectric performance of Sb (III) doped $Bi_2(Te_{1-x}Se_x)_3$ thin films.*

Film Composition	S (μVK^{-1})	ρμΩm	Thermal Conductivity ($Wm^{-1}K^{-1}$)	PF ($mWK^{-}m^{-}$)	ZTat 300K
D_1:$Bi_{1.98}$ $Sb_{0.02}(Te_{0.5}Se_{0.5})_3$	115	32.51	0.255	4.06	0.312
D_2:$Bi_{1.96}$ $Sb_{0.04}(Te_{0.5}Se_{0.5})_3$	129	37.76	0.353	5.12	0.363
D_3:$Bi_{1.94}Sb_{0.06}$ $(Te_{0.5}Se_{0.5})_3$	147	43.74	0.361	6.60	0.410
D_4:$Bi_{1.92}Sb_{0.08}$ $(Te_{0.5}Se_{0.5})_3$	158	50.78	0.391	7.62	0.418
D_5:$Bi_{1.90}Sb_{0.1}$ $(Te_{0.5}Se_{0.5})_3$	**168**	**58.30**	**0.364**	**8.67**	**0.569**

4. Conclusion

It is concluded that Sb(III) doped $Bi_2(Te_{1-x}Se_x)_3$ thin film was successfully deposited by APT and characterized by optostructural, morphological and electrical studies. The UV-Vis-NIR spectrum of the films reveals that the deposited films having band gap in the range of 1.46 to 1.89 eV. The XRD of the film shows rhombohedral structure. SEM shows that films are compact, uniform and adhrent with pin-hole-free nature. From EDAX the compositions of the films are in good stoichiometric ratio. Electrical and TEP study shows Sb(III) doping in $Bi_2(Te_{1-x}Se_x)_3$ mixed metal chalcogenide thin films are semiconducting having p-type conduction mechanism. The highest figure of merit obtained was 0.312 and 0.569 for D_1 to D_5 samples. These properties revels that the Sb (III) doping in $Bi_2(Te_{1-x}Se_x)_3$ thin film material is suitable material for thermo cooling devices. 86, 1634 (1999).

References

[1] A. Purkayastha, A. Jain, C. Hapenciuc, R. Buckley, B. Singh, C. Karthik, R. Mehta, T. Borca-Tasciuc, G. Ramanath, Chem. Mater., 23, 3029 (2011).

[2] S. V. Ovsyannikov, Yu. A. Grigor'eva, G. V. Vorontsov, L. N. Luk'yanova, V. A. Kutasov, V. V. Shchennikov, Phys. Solid State, 54, 261 (2012).

[3] W. Wang, B. Poudel, J. Yang, D. Z. Wang, and Z. F. Ren, J. Am. Chem. Soc., 127, 13792 (2005).

[4] D. D. Frari, S. Dilibereto, N. Stein, C. Boulanger, J. M. Lecuire, 483,44(2005).

[5] K. Wojciechowski, E. Godlewska, K. Mars, R. Mania, G. Karpinski, P. Ziolkowski, C. Stiewe, E. Muller, Vacuum, 82, 1003 (2008).

[6] L. N. Lukyanova, V. A. Kutasov, P. P. Konstantinov, & V. V. Popov, J. Electronic Mater.,39, 2070 (2010).

[7] V. A. Kutasov and L. N. Luk'yanova, Fiz. Tverd. Tela, Phys., Solid State, 48, 2289 (2006).

[8] L. N. Lukyanova, V. A. Kutasov, and P. P. Konstantinov, Fiz. Tverd. Tela, Phys. Solid State, 47, 233(2005).

[9] H. Noro, K. Sato, and H. Kagechika, J. Appl. Phys. 73, 1252 (1993).

[10] C. Navone, M. Soulier, M. Plissonnier and A. L. Seiler, J. Electronic Mater., 39, 1755(2010).

[11] B. S. Farag, A. M. Abou EL Soud, H. A. Zayed, S. A.Gad, J. Ovonic Research, 6, 267 (2010).

[12] S. M. Patil, S. R. Mane, R. M. Mane, S. S. Mali, P. S. Patil, P. N. Bhosale, Canadian J. Chemistry, 89, 1375(2011).

[13] R.M. Mane, S.R. Mane, R. R. Kharade, P.N. Bhosale, J. Alloys Compds., 491, 321(2010).

[14] M. M. El-Samanoudy, Thin Solid films 423, 201, (2003).

[15] P. Lostak, C. Drasar, H. Sussmann, P. Reinshaus, R. Novotny and L. Benes, J. Cry. Growth, 179, 144 (1997).

[16] N. S. Patil, A. M. Sargar, S. R. Mane, P. N. Bhosale, Appl. Surface Sci., 254, 5261 (2008).

[17] L. N. Lukyanova, V. A. Kutasov, V. V. Popov, P. P. Konstantinov, Semiconductors and dielectrics, 46, 1404 (2004).

[18] C. A. Bridges, J. E. Greedan, Holger Kleinke, Solid State Chem., 177, 4516 (2004).

[19] A. Datta, J. Paul, A. Kar, A. Patra, Z. Sun, L. Chen, J. Martin, G. S. Nolas, J. Cryt. Growth Design. 10, 3983 (2010).